

CRS-partial stack and spectral content

Felipe A. V. Pena, Lourenildo W. B. Leite and Wildney W. S. Vieira, UFPA, Brazil

Copyright 2013, SBGF - Sociedade Brasileira de Geofísica.

This paper was prepared for presentation at the 13th International Congress of the Brazilian Geophysical Society, held in Rio de Janeiro, Brazil, August 26-29, 2013.

Contents of this paper were reviewed by the Technical Committee of the 13th International Congress of The Brazilian Geophysical Society and do not necessarily represent any position of the SBGF, its officers or members. Electronic reproduction or storage of any part of this paper for commercial purposes without the written consent of The Brazilian Geophysical Society is prohibited.

Abstract

This work had as a general aim at the application of techniques based on the common-reflection-surface stack (CRS), and a specific aim at trace interpolation using the CRS-partial stack in order to analyse the effect on spatial aliasing to guarantee that the total spectrum content be limited to the two main spectral quadrants. For this, two synthetic tests were constructed that stayed close to the paraxial ray theory, and to validate the hypotheses, by deleting traces, reconstruction of section, and the addition of noise.

Introduction

The quality of reflection seismic data is an important aspect in seismic processing and imaging, and part of its analysis is performed in the spectral domain, starting with the field survey parameters, the processing, the velocity analysis, the inversion and up the migration. Factors like the inhomogeneities in the subsurface, the presence of fault structures and strong velocity contrasts lead to a decrease of the S/N ratio and to a more complicated work flow to precondition the data for velocity analysis, velocity model building, and other processes (Baykulov and Gajewski, 2007). Regularization of seismograms and filling the gaps in cases of missing data usually are performed using different binning and interpolation techniques, as described, for instance, by Brune et al. (1994), Yilmaz (2000), and Fomel (2003).

This research topic is part of the CRS stack method, as described by Müller (1999), Jäger (1999) and Mann (2002), to improve both the quality of the pre-stacked and stacked sections as measured by the spectrum content by a consistent interpolation process. According to Müller (1999) and Jäger (1999) the CRS stacking surface approximates the traveltimes of seismic reflection data more accurately than NMO/DMO stack; therefore, the application of the CRS stacking surface to produce regularized data can be superior to methods based on the conventional techniques of NMO/DMO and binning/interpolation as described by Brune et al. (1994).

CRS stack

The CRS stack method simulates a zero-offset (ZO) section from multi-coverage seismic reflection data for 2-D media without explicit knowledge of the macro-velocity

model.

The CRS stack surface, as illustrated in Figure 1, is an operator that approximates the true subsurface reflector by a reflector element that locally has the same curvature as the true reflector. The traveltimes of primary reflection events is described by three parameters, α , R_N and R_{NIP} , in the hyperbolic form, as:

$$t^2(x_m, h) = \left(t_0 + 2 \frac{\sin \alpha_0}{v_0} (x_m - x_0) \right)^2 + 2t_0 \frac{\cos^2 \alpha_0}{v_0} \left(\frac{(x_m - x_0)^2}{R_N} + \frac{h^2}{R_{NIP}} \right). \quad (1)$$

The emergence position is defined by the point $P_0(x_0, t_0)$. Operator (1) is a function of the independent spatial common midpoint x_m coordinate, and of the half source-receiver offset h . The quantity v_0 is a velocity established near the surface and around P_0 , and t_0 the ZO, or normal incidence, traveltimes. The emergence ray is characterized by the vertical incidence angle α , and by the radius of curvature of the Normal (N) wave, R_N , and of the normal-incidence-point (NIP) wave R_{NIP} .

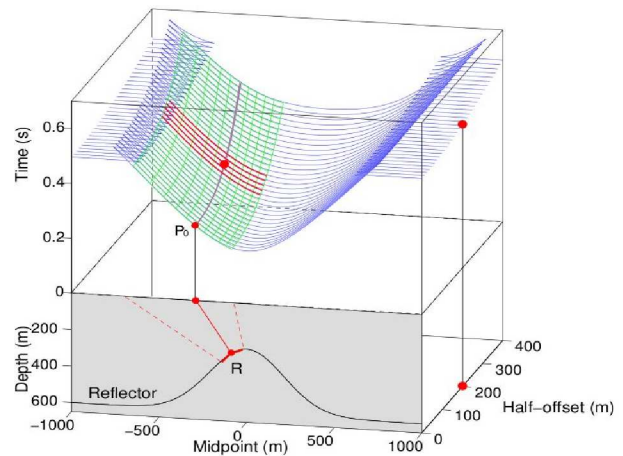


Figure 1: The CRS stack sums the data along the green surface, and assigns the result to the point P_0 . The CRS-partial stack performs the summation of data around the specified point on a CMP traveltime curve (magenta line), and assigns the result to that point in a new generated CRS to form the supergather. The CRS-partial stack surface is shown in red, and coincides locally with the CRS stack surface. Baykulov (2009)

The CRS-partial stack, described by Baykulov and Gajewski (2007), aims at to interpolate traces in a CMP, to increase the signal-noise in the pre-stacked data, and consequently to improve on the aliasing limits. Partial CRS stack calculates a stacking surface around a specified point defined by its offset and traveltimes coordinates in a chosen CMP location, and performs the summation of data along

that surface. Repeating this procedure for all desired points generates a new gather to compose the CRS supergather.

Figure 1 shows the stack and data surfaces, and the point $P_0(x_0, t_0)$ where the results are placed.

The estimation of the CRS parameters is described by Müller (1999), and performed in optimization steps using special cases of the operator (1) that is controlled by the CRS parameters. The tri-parametric search is performed in the semblance domain, and the operator is split into simpler problems involving one or two unknown parameters.

The CRS-parcial stack surface is computed for a specified CMP, and for all samples $A(t_A, h_A)$, where t_A is the traveltme, and h_A is the half offset. For this, the ZO traveltme, and the corresponding CRS parameters (α, R_N, R_{NIP}) describing that event must be calculated.

This search for the CRS attributes is simplified to find the hyperbole of the CMP that best fits the sample A of the event (see Figure 2). Therefore all zero-offset traveltmes within the range $[0; t_A]$ and the corresponding CRS parameters are tested to determine the hyperbola that has the minimum time deviation from t_A at the offset h_A .

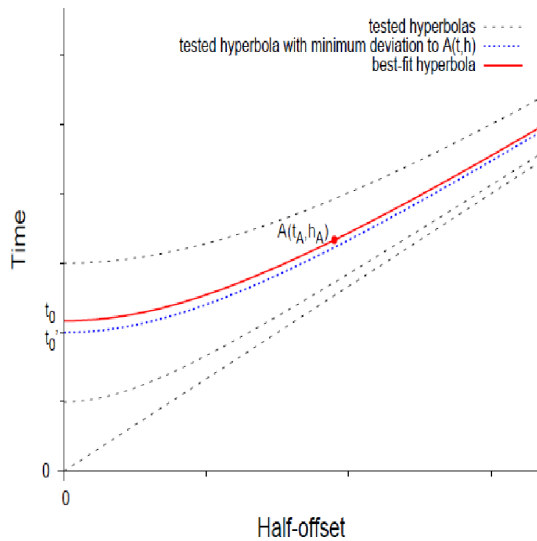


Figure 2: Traveltime curves tested in the search for a best hyperbola $A(t_A, h_A)$ fit.

Time t'_0 corresponds to the minimum deviation between the computed and the observed traveltme for sample A , and the correct t_0 time is computed using the CRS parameters for best fit the traveltme of the A element. The t_0 is found by equation (2) derived from equation (1) after solving the quadratic equation with $m = 0$, and neglecting the negative solution for t_0 .

$$t_0 = -\frac{h_A^2 \cos^2 \alpha}{V_0 R_{NIP}} + \sqrt{\left(\frac{h_A^2 \cos^2 \alpha}{V_0 R_{NIP}}\right)^2 + t_A^2}, \quad (2)$$

Substituting the t_0 time from equation (2) in equation (1) yields the traveltme formula for partial CRS stacking surface shown in equation (3) with the CRS parameters

corresponding to t'_0 :

$$t^2(x_m, h) = \left(-\frac{h_A^2 \cos^2 \alpha}{V_0 R_{NIP}} + \sqrt{\left(\frac{h_A^2 \cos^2 \alpha}{V_0 R_{NIP}}\right)^2 + t_A^2} + \frac{2 \sin \alpha}{V_0} (x_m - x_0) \right)^2 + \frac{2 \cos^2 \alpha}{V_0} \left(-\frac{h_A^2 \cos^2 \alpha}{V_0 R_{NIP}} + \sqrt{\left(\frac{h_A^2 \cos^2 \alpha}{V_0 R_{NIP}}\right)^2 + t_A^2} \right) \left(\frac{(x_m - x_0)^2}{R_N} + \frac{h_A^2}{R_{NIP}} \right). \quad (3)$$

This surface is used to sum up the data coherently. The resulting sum is divided by the number of traces involved in the summation. So, the amplitudes of signal in the generated CRS supergather are comparable with the amplitudes of signal in the CMP gathers, whereas the noise is attenuated.

Results and Conclusions: Sparse Data test

The constructed model to simulate a geological environment used in the tests was based on the description of Duvencek (2004), and consists of homogeneous and isotropic layers bounded by smooth curved interfaces. The blocky model is of Figure 3, where the velocities vary from 2000m/s at the top to 5000m/s at the lowerpart.

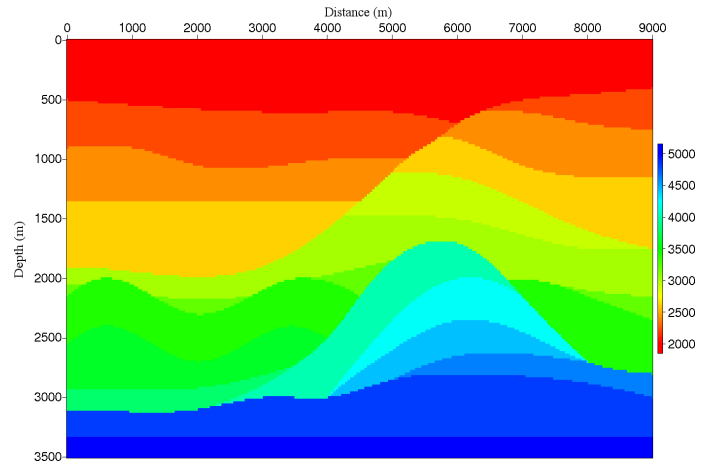


Figure 3: Block velocity model.

In the sparse data test, random elimination of traces of done using the program *sukill* by zeroing 80 % of the original traces. Figure 4 shows an example of the CMP 200 that is displayed before and after the random elimination, where only 6 of 30 traces were kept in the process. This sparse data was used as input on the automatic search of the CRS attributes to be used in the stack. The aperture used for the partial CRS was $(-1475$ to $+1475)$, and the midpoint displacement was 200m for the traveltme 0.3s to 300m for 2.7s.

In the mechanism to perform the CRS-partial stack, one can use only positive or negative offsets at a time. As the configuration of the data acquisition was split-spread, the process is performed in two steps; once for positive offsets, and another for negative offsets, and then concatenate the results.

Figure 5 shows the result in the CMP gather 200 before

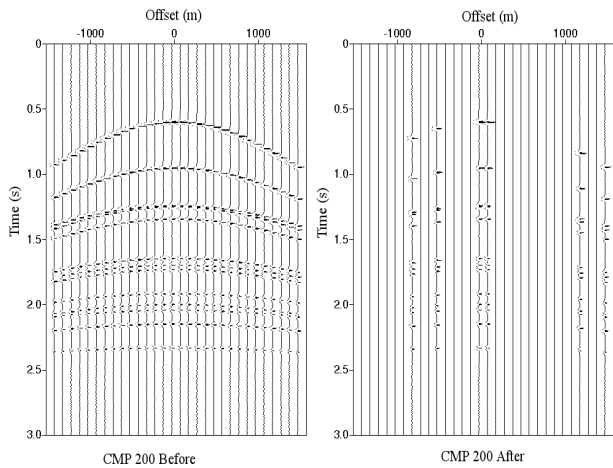


Figure 4: CMP gather 200 before and after the elimination of traces.

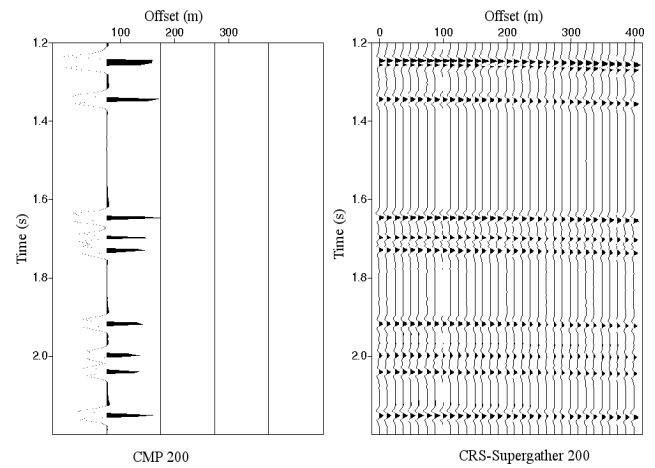


Figure 6: Detail images of CMP gather 200 before and after of partial CRS stacked.

and after of the CRS-partial stack, where one can see the improvement in the signal/noise ratio by the visualization of seismic events. Figure 6 shows a detail time-space window of 1s and 400m, in order to observe the CRS-partial improvement in the continuity of events, and the gaps filled in the pre-stacked data.

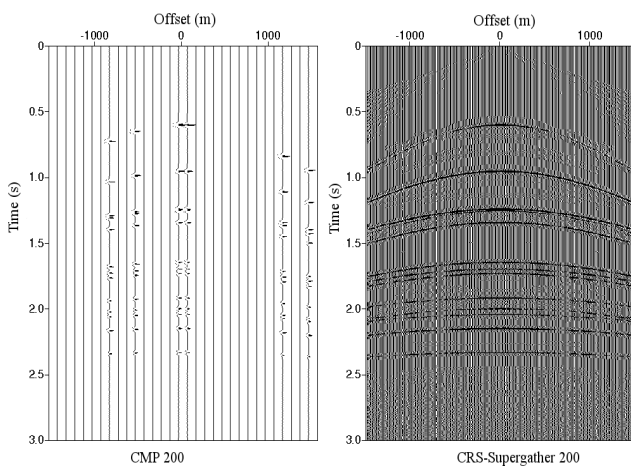


Figure 5: CMP gather 200 before and after the partial CRS stacked.

Figure 7 shows the f-k spectrum of CMP gather 200 which shows the spectrum contamination. The spatial Nyquist frequency is 0.02 cycle/meter, and the temporal Nyquist frequency is 125 Hz.

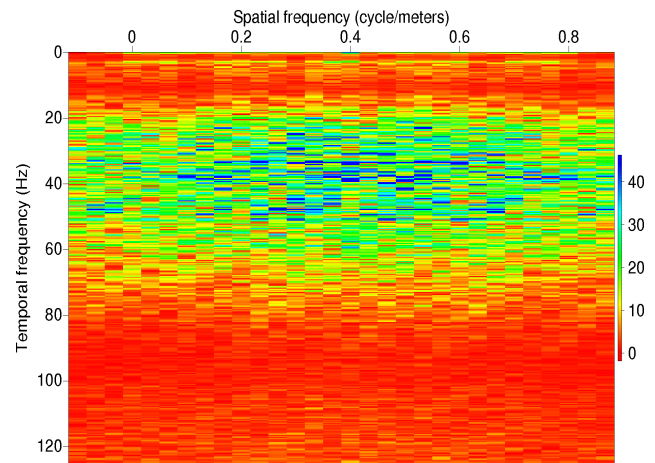


Figure 7: f-k spectrum of CMP gather 200 before of partial CRS stacked.

After CRS-partial stack process, the spectrum shown in Figure 8 was calculated, and it shows that the spectrum content is better limited to the two quadrants. This is obtained only by the increase of the Nyquist spatial frequency to 0.08 cycle/meters, what results in diminishing aliasing contamination.

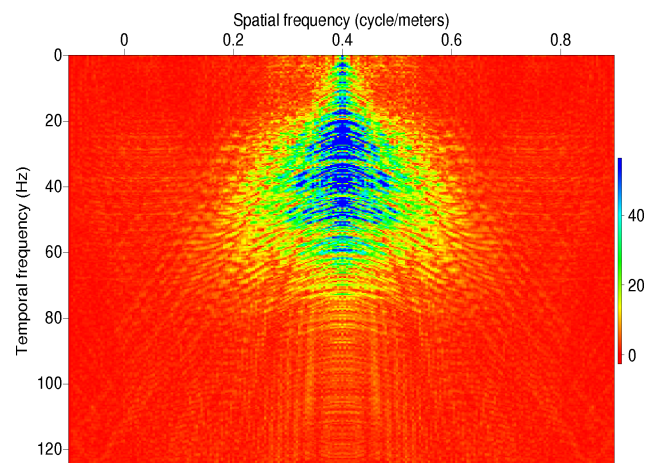


Figure 8: f-k spectrum of CMP gather 200 after CRS-partial stack.

To analyze the advantages resulting from the application of CRS-partial stack, different stacks were compared. The first is the automatic CMP stack shown in Figure 9, where you can see many discontinuities in the section. The second in Figure 10, the conventional CRS-stack

which does not use the CRS-partial stack, which shows considerable improvement with respect to Figure 9. The third in Figure 11 shows the CRS-supergather stack, where

a better continuity of events than in Figures 9 and 10.

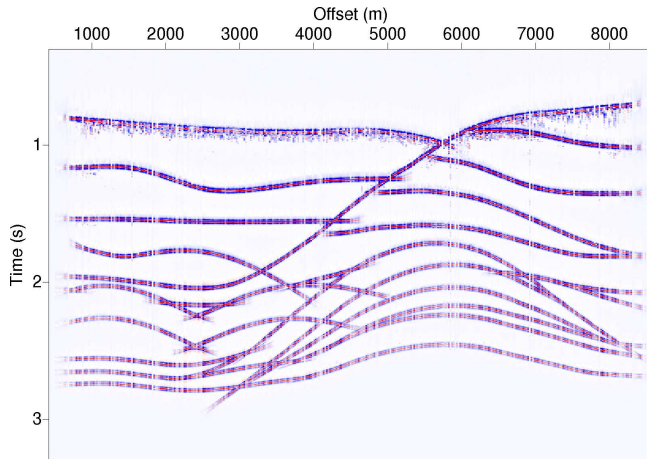


Figure 9: CMP-automatic stack.

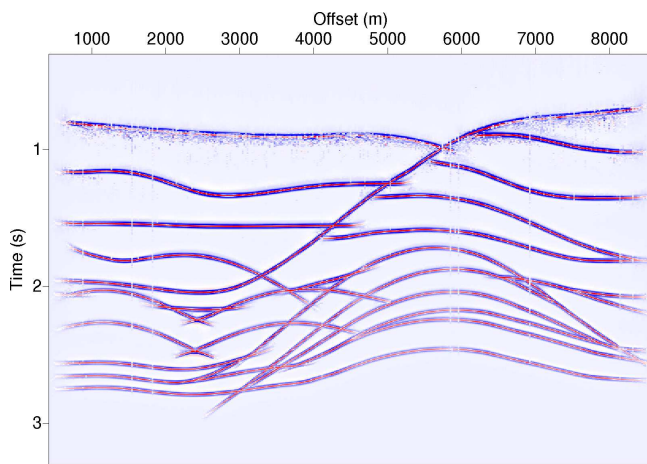


Figure 10: CRS-conventional stack.

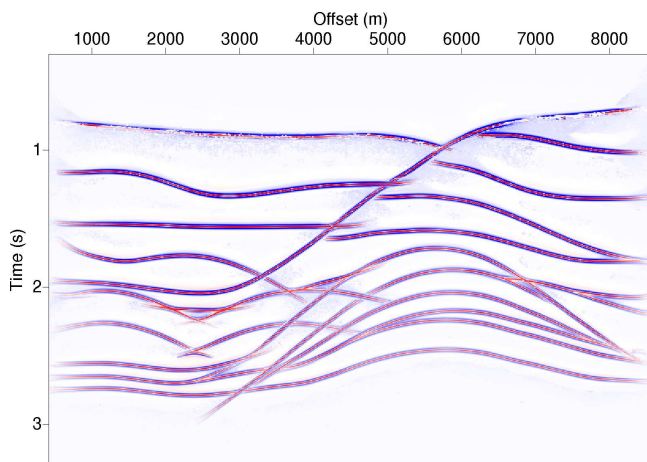


Figure 11: CRS-supergather stack.

Because the partial CRS stack performs the summation of data to generate one sample in the CRS supergather,

it enhances the quality of the seismograms by increasing their S/N. Moreover, taking into account information from the neighboring traces allows us to fill data gaps.

Results and Conclusions: Additive noise test

In this part we have systematically repeated all the process steps of the above section, in order to analyse the CRS-partial stack with respect to noise addition. For this purpose a Gaussian $S/N = 05$ was applied in the pre-stacked data using the program *sunoise*. The results shown in Figure 12, before and after the addition of noise in the CMP gather, where events are better seen in the upper part of the figure with noise.

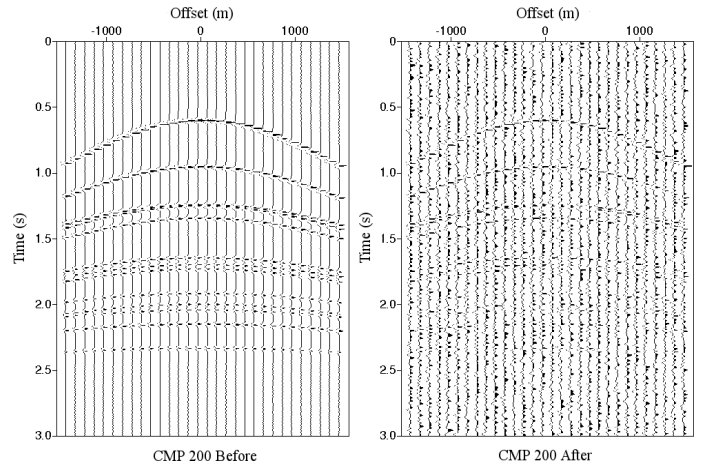


Figure 12: CMP gather 200 before and after noise addition.

This noisy data was used as input for the automatic CRS attribute search. The aperture used for the partial CRS was (-1475 to +1475), with 200m for the traveltim of 0.3s to 300m in 2.7s.

The result of the CRS-partial stack is shown in Figure 13 with a better S/N ratio, under a better continuity of reflections compared to CMP gather.

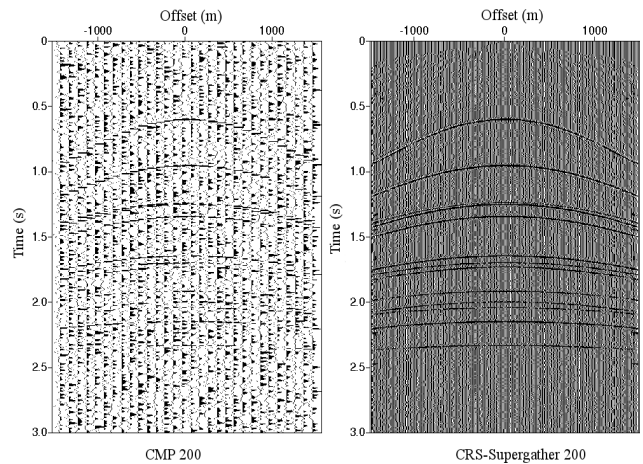


Figure 13: CMP gather 200 before and after the CRS-partial stack.

Details are shown in Figure 14. Compared to the CMP-conventional gather, the reflections in the CRS-supergather

are better visible, where noise is present, but the aspect of the S/N ratio increased significantly.

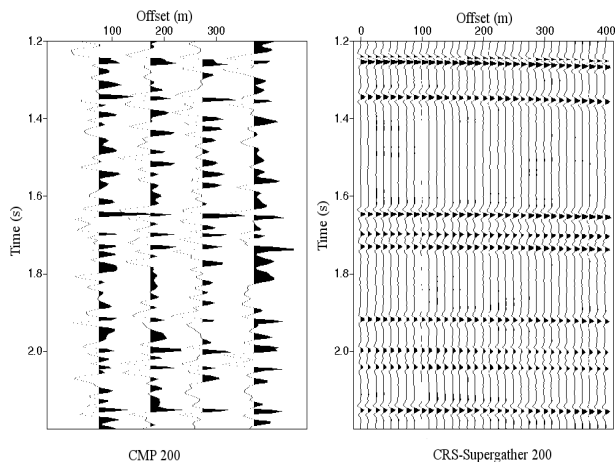


Figure 14: Detail of the CMP gather 200 before and after CRS-parcial.

Figure 15 shows the f-k spectrum of CMP gather 200 before and after CRS-parcial stack, where the temporal Nyquist frequency is 125Hz and the Nyquist spatial frequency is 0.02cycle/meter.

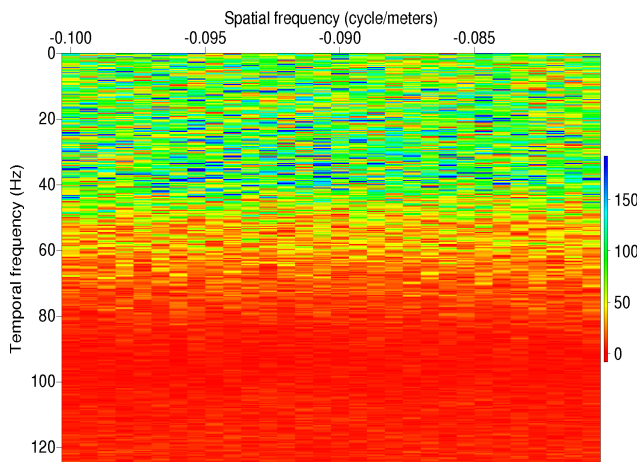


Figure 15: f-k spectrum of CMP gather 200 before CRS-parcial stack.

Figure 16 shows the f-k spectrum of CMP gather 200 after CRS-parcial stack, where the spatial frequency of Nyquist increased to 0.08 cycle/meter, thus diminishing aliasing effect to contain the spectrum in two quadrants. The Nyquist temporal frequency remains the same, 125Hz.

Figure 17 shows the section of CMP-automatic stack, where despite the noise present, reflectors are visible.

Figure 18 shows the CRS-conventional stack, with a slight increase in the S/N ratio, and highlighting the deeper reflectors compared to Figure 17.

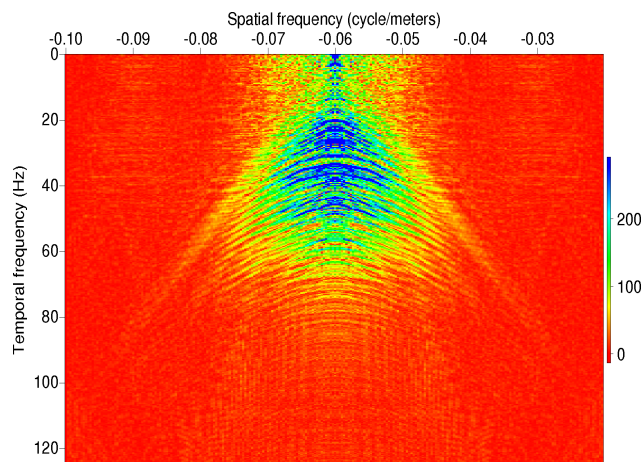


Figure 16: f-k spectrum of CMP gather 200 after CRS-parcial stack.

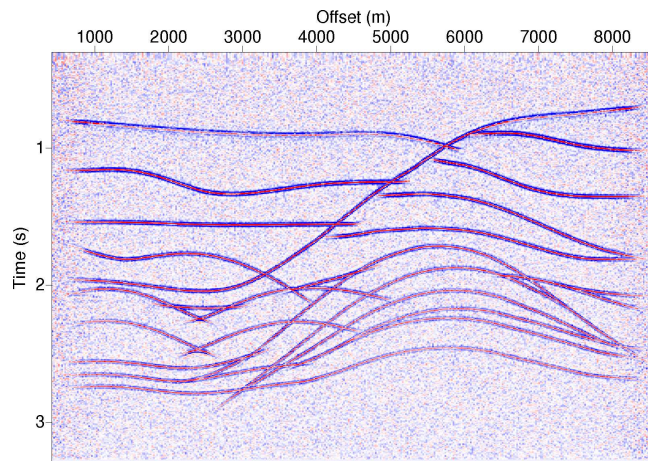


Figure 17: CMP-automatic stack.

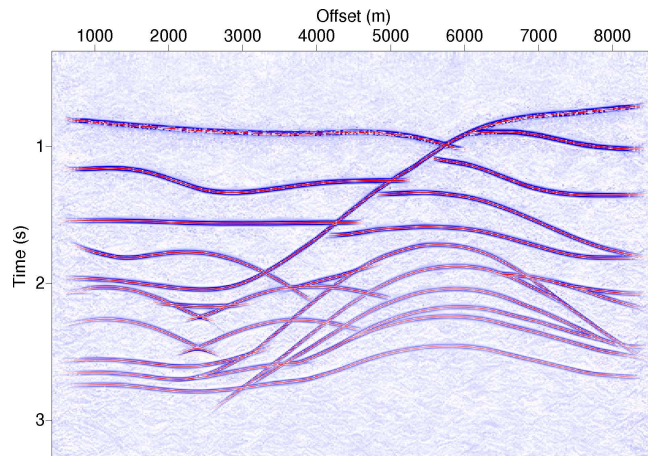


Figure 18: CRS-conventional stack.

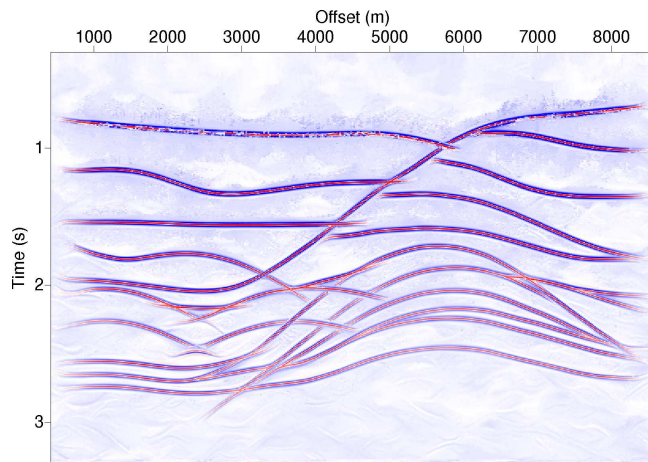


Figure 19: CRS-supergather stack.

Figure 19 shows the CRS-supergather stack with better S/N ratio compared to Figures 17 and 18. This means that the CRS-partial stack is very stable to the presence of noncoherent noise.

So we recommend using the partially stacked gathers instead of conventional CMPs, especially for sparse data of low quality. Results of velocity analysis, stacking, and depth migration might be improved using gathers generated by the new approach. The improved CRS parameter sets might be used further by NIP-wave tomographic inversion.

References

- Baykulov, M., and Gajewski, D., 2007, Prestack seismic data enhancement with crs parameters: WIT, , no. 11, 50–61.
- Baykulov, M., 2009, Seismic imaging in complex media with the common reflection surface stack: Master's thesis, Hamburg.
- Brune, R. H., O'Sullivan, B. L., and Lu, L., 1994, Comprehensive analysis of marine 3-d bin coverage: *The Leading Edge*, **21**, 1010–1015.
- Duveneck, E., 2004, Tomographic determination of seismic velocity models with kinematic wavefield attributes: Ph.D. thesis, Karlsruhe University, Karlsruhe.
- Fomel, S., 2003, Seismic reflection data interpolation with differential offset and shot continuation: *Geophysics*, **68**, 733–744.
- Jäger, R., 1999, The common-reflection-surface stack: Master's thesis, Karlsruhe University, Karlsruhe.
- Mann, J., 2002, Extensions and applications of the common reflection surface stack method: Ph.D. thesis, Karlsruhe University, Karlsruhe.
- Müller, T., 1999, The common reflection surface stack method-seismic imaging without explicit knowledge of the velocity model: Ph.D. thesis, Karlsruhe University, Karlsruhe.
- Yilmaz, O., 2000, Seismic data analysis, volume 1 Society of Exploration Geophysicists, Tulsa, OK.

Acknowledgments

The authors would like to thank the Brazilian institutions UFPA (*Universidade Federal do Pará*), CNPq and in special to the National Institute of Science and Technology (*Instituto Nacional de Ciência e tecnologia*), INCT-GP.